ORIGINAL PAPER

A highly active FeNi₃–SiO₂ magnetic nanoparticles catalyst for the preparation of 4H-benzo[b]pyrans and Spirooxindoles under mild conditions

Mohammad Ali Nasseri · Seyed Mohsen Sadeghzadeh

Abstract A green and efficient method for the synthesis of various 4H-benzo[b]pyrans and Spirooxindoles in the presence of FeNi₃–SiO₂ as the nanocatalyst at room temperature is reported. High catalytic activity and ease of recovery from the reaction mixture using an external magnet, and several reuse times without significant losses in performance are additional eco-friendly attributes of this catalytic system.

Keywords FeNi₃–SiO₂ · 4H-benzo[b]pyrans · Spirooxindoles · Magnetic nanoparticles (MNPs) · Green chemistry · One-pot synthesis

Introduction

4H-Benzo[b]pyrans and Spirooxindoles are an important class of compounds which have received considerable attention in recent years due to their wide range of biological activities. Compounds with these ring systems have diverse pharmacological activities [1–5]. Consequently, numerous methods have been reported from the synthesis of 4H-Benzo[b]pyrans. A variety of reagents such as, HMTAB [6], TEBA [7], RE(PFO)3 [8], NaBr [9], (S)-proline [10], the use of microwave irradiation [11], KF-basic alumina under ultrasound irradiation [12], and amino-functionalized

ionic liquid [13] were found to catalyze these reactions, and catalysis including ammonium chloride [14], ethylenediamine diacetate [15], surfactant metal carboxylates [16], L-proline [17], triethylbenzyl ammonium (TEBA) salt [18], and b-cyclodextrin [19] can also catalyze the synthesis of various Spirooxindoles. However, some of the reported methods have the following drawbacks: for example, use of expensive reagents, long reaction times, low yields of products, and use of an additional microwave oven.

Many solid catalysts have been traditionally synthesized in nano size per se or as nano materials inside a porous matrix. Silica has been employed as both supports and catalysts [20–26]. Among these, silica has resurfaced to the fore as a solid acid catalyst due to its important characteristics such as, particle size, surface chemistry, particle shape, surface area, and other properties that are overwhelmingly used as nanocatalyst or support for dispersing active centers and reagents [27–31]. Nanocatalysts have also been widely used for the organic synthesis in both homogeneous and heterogeneous conditions [32–35].

The superparamagnetic nanoparticles, whose flocculation and dispersion can be reversibly controlled by applying a magnetic field, were recently employed in the catalytic applications and received the immense attractions as a new type of the recyclable support matrix. In the absence of the external magnetic field, superparamagnetic nanoparticles can be well dispersed in a reaction solution, providing large surface area, which can be readily accessed by substrate molecules [36]. Most importantly, the MNP-supported catalyst could be recollected by using an external magnet conveniently without filtration or centrifugation. We have used these newly synthesized FeNi₃–SiO₂ as a magnetically recyclable nanocatalyst for the efficient one-pot synthesis of 4H-Benzo[b]pyrans and Spirooxindoles at room temperature with good to excellent yield (Schemes 1, 5).

M. A. Nasseri (✉) · S. M. Sadeghzadeh
Department of Chemistry, College of Sciences,
Birjand University, P.O. Box 97175-615, Birjand, Iran
e-mail: mohammadali.nasseri@yahoo.com

Scheme 1 Synthesis of 4H-benzo[b]pyrans from 1,3-Diketones, aldehydes, and malononitrile in the presence of FeNi$_3$–SiO$_2$
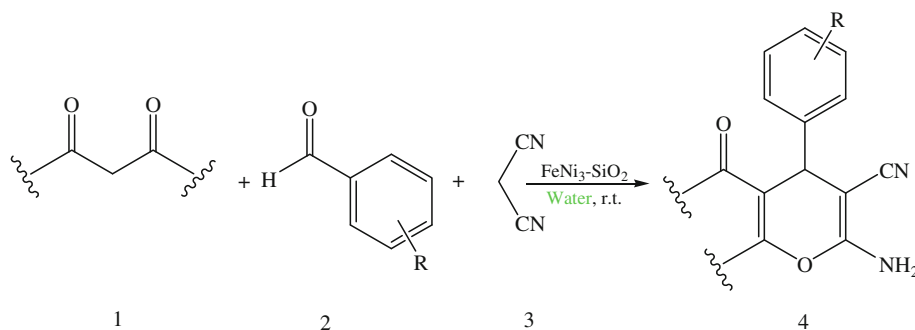
Experimental

Materials and methods

Chemical materials were purchased from Fluka and Merck in high purity. Melting points were determined in open capillaries using an Electrothermal 9100 apparatus and are uncorrected. FTIR spectra were recorded on a VERTEX 70 spectrometer (Bruker) in the transmission mode, in spectroscopic grade KBr pellets for all the powders. The particle size and structure of FeNi$_3$–SiO$_2$ MNPs were observed by using a Philips CM10 transmission electron microscope operating at 100 kV. Powder X-ray diffraction data were obtained using Bruker D8 Advance model with Cu ka radiation. NMR spectra were recorded in DMSO on a Bruker Advance DRX-400 MHz instrument spectrometer using TMS as internal standard. The purity determination of the products and reaction monitoring were accomplished by TLC on silica gel polygram SILG/UV 254 plates. Mass spectra were recorded on Shimadzu GCMS-QP5050 mass spectrometer.

General procedure for the preparation of FeNi$_3$ nanoparticles

The synthesis procedure is illustrated as follows: (1) 0.01 mol FeCl$_2$·4H$_2$O and 0.03 mol NiCl$_2$·6H$_2$O were dissolved into 200-mL distilled water, followed by the addition of PEG (1.0 g, MW 6000). (2) Sodium hydroxide (NaOH) was added to the solution and the pH value was controlled in the range $12 \leq \text{pH} \leq 13$. (3) Different amount of hydrazine hydrate (N$_2$H$_4$·H$_2$O, 80 % concentration) was added to the above suspension. The reaction was continued for about 24 h at room temperature. During this period, the pH value was adjusted by NaOH and kept in the range $12 \leq \text{pH} \leq 13$. The black FeNi$_3$ MNPs were then rinsed several times with ionized water [37].

General procedure for the preparation of FeNi$_3$–SiO$_2$ nanoparticles

0.02 mol of FeNi$_3$ MNPs were dispersed in a mixture of 80 mL of ethanol, 20 mL of deioned water, and 2.0 mL of 28 wt % concentrated ammonia aqueous solution (NH$_3$·H$_2$O), followed by the addition of 0.20 g of tetraethyl orthosilicate (TEOS). After vigorous stirring for 24 h, the final suspension was repeatedly washed, filtered for several times, and dried at 60 °C in the air (Fig. 1) [37].

Characterization of catalyst

TEM images of FeNi$_3$ and FeNi$_3$–SiO$_2$ MNPs are shown in Fig. 2. The average size of FeNi$_3$ MNPs is about 25 nm (Fig. 2a). After being coated with a silica layer, the typical core–shell structure of the FeNi$_3$–SiO$_2$ MNPs can be observed. The dispersity of FeNi$_3$–SiO$_2$ MNPs is also improved, and the average size increases to about 50 nm (Fig. 2b). Figure 3 shows the XRD pattern of FeNi$_3$–SiO$_2$ nanoparticle particles synthesized with [N$_2$H$_4$·H$_2$O]/[FeNi$_3$] molar ratio of 24:1. It can be seen that three characteristic peaks for (FCC)-FeNi$_3$ ($2\theta = 44.3$, 51.5, 75.9) from (111) (200) and (220) planes, are obtained. No XRD peaks for α-Fe (i.e., at 2θ of 65.2) and (FCC)-Ni (i.e., at 2θ of 44.5, 51.8, and 76.4) can be observed. Besides the peak of FeNi$_3$, the XRD pattern of FeNi$_3$–SiO$_2$ core–shell nanoparticles presented a broad featureless XRD peak at low diffraction angle, which corresponded to the amorphous state SiO$_2$ shells (JCPDS card No. 29-0085).

General procedure for the synthesis of 4H-benzo[b]pyrans

A mixture of 1,3-Diketone (1 mmol), aldehyde (1 mmol), malononitrile (1 mmol), and FeNi$_3$–SiO$_2$ MNPs (0.0007 g) in water (5 mL) was stirred at room temperature for 10–20 min (the progress of the reaction was monitored by TLC). After completion, the reaction mixture was filtered
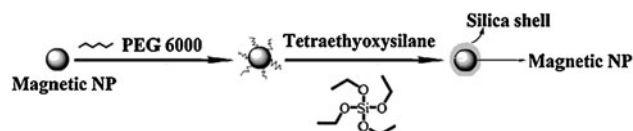

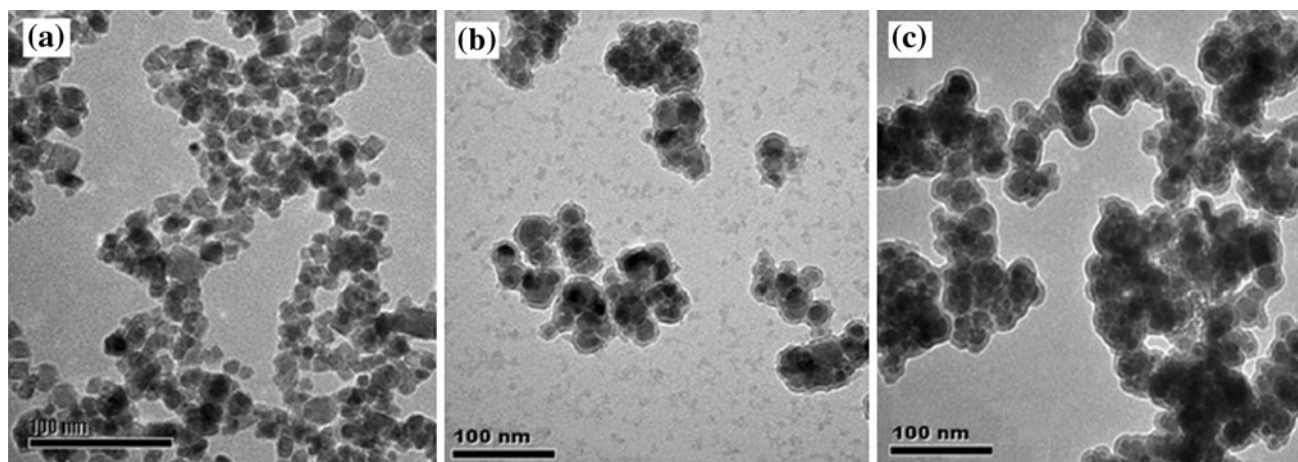**Fig. 1** Schematic illustration of the synthesis for FeNi$_3$–SiO$_2$ nanoparticles

Fig. 2 TEM images of **a** FeNi$_3$, **b** FeNi$_3$-SiO$_2$ before use (**b**) and after reuse ten times. High agglomeration of FeNi$_3$–SiO$_2$ can not be seen (**c**)
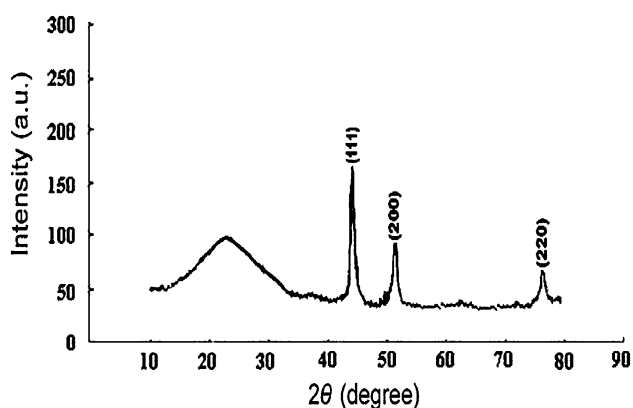

Fig. 3 XRD pattern of FeNi$_3$–SiO$_2$ MNPs synthesized with [N$_2$H$_4$·H$_2$O]/[FeNi$_3$] ratio of 24:1

and the precipitate washed with H$_2$O (5 mL) and EtOH (5 mL) to afford pure 4H-benzo[b]pyrans.

General procedure for the synthesis of Spirooxindoles

A mixture of 1,3-Diketone (1 mmol), isatin (1 mmol), malononitrile (1 mmol), and FeNi$_3$–SiO$_2$ MNPs (0.0007 g) in water (5 mL) was stirred at room temperature for 10–15 min. The precipitated solid was filtered, washed with water followed by washing with a mixture of ethyl-acetate/hexane (20:80), and then dried under vacuum. The product obtained was further purified by recrystallization from hot ethanol.

Results and discussion

The effect of solvent on this reaction was examined and the obtained results are summarized in Table 1. In n-Hexane, CHCl$_3$, and Dioxane (Table 1, entries 12–14), only a trace

of product was observed. On the contrary, moderate yields could be achieved when other organic solvents were applied as the solvent (Table 1, entries 2–10). More strikingly, we found that the reaction proceeded smoothly in water and gave the desired product of 97 % yield (Table 1, entry 1).

At this stage, the amount of catalyst necessary to promote the reaction efficiently was examined (Fig. 4). It was observed that the variation for FeNi$_3$–SiO$_2$ MNP had an effective influence. The best amount of FeNi$_3$–SiO$_2$ MNP is 0.0007 g which afforded the desired product in 97 % yields (Fig. 4).

It is important to note that the magnetic property of FeNi$_3$–SiO$_2$ facilitates its efficient recovery from the reaction mixture during work-up procedure (Fig. 5). The activity of the recycled catalyst was also examined under the optimized conditions. After the completion of reaction, the catalyst was separated by an external magnet, washed with methanol, and dried at the pump. The recovered catalyst was reused for ten consecutive cycles without any significant loss in catalytic activity (Fig. 6). The FeNi$_3$–SiO$_2$ before use does not result in the change of the morphology and size of the obtained FeNi$_3$–SiO$_2$ after reuse (Fig. 2c).

To show the unique catalytic behavior of FeNi$_3$–SiO$_2$ MNPs in these reactions, we have performed one-pot reaction of benzaldehyde (compound 2a), 5,5-dimethyl-cyclohexane-1,3-dione (compound 1a), and malononitrile (compound 3) in the presence of Na$_2$SeO$_4$, Tetra-methyl ammonium hydroxide, Nanosized Ce$_1$Mg$_x$Zr$_{1-x}$O$_2$, NaBr, and MgO (Table 2). As it is evident from Table 2, FeNi$_3$–SiO$_2$ is the most effective catalyst for this purpose, leading to the formation of 4H-benzo[b]pyran (compound 4a) in a lesser time with better yield and reduces the amount of catalyst. The increased catalytic activity of FeNi$_3$–SiO$_2$ over the another catalysts may be attributed to the higher surface area of SiO$_2$.

Table 1 Solvent screening for the reaction between 5,5-dimethyl-cyclohexane-1,3-dione, benzaldehydes, and malononitrile

Entry	Solvent	Yield (%)[a]
1	H_2O	97
2	EtOH	78
3	CH_3CN	60
4	THF	40
5	CH_2Cl_2	40
6	Toluene	20
7	EtOAC	75
8	MeOH	85
9	DMF	64
10	DMSO	70
11	Solvent free	76
12	n-Hexane	Trace
13	$CHCl_3$	Trace
14	Dioxane	Trace

Reaction conditions: 5,5-dimethyl-cyclohexane-1,3-dione (1 mmol), malononitrile (1 mmol), benzaldehyde (1 mmol), solvent (10 mL), $FeNi_3$–SiO_2 (0.001 g) at room temperature for 40 min

[a] Isolated yields
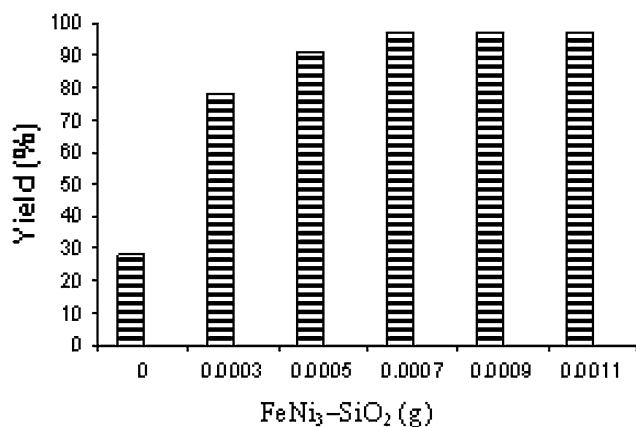
Fig. 4 Effect of increasing amount of $FeNi_3$–SiO_2 on the preparation of 4H-benzo[b]pyran (reaction of 5,5-dimethyl-cyclohexane-1,3-dione, benzaldehyde and malononitrile in the presence of $FeNi_3$–SiO_2 at room temperature in water)

Fig. 5 **a** Reaction mixture. **b** Separation of $FeNi_3$–SiO_2 from the reaction mixture by an external magnetic field
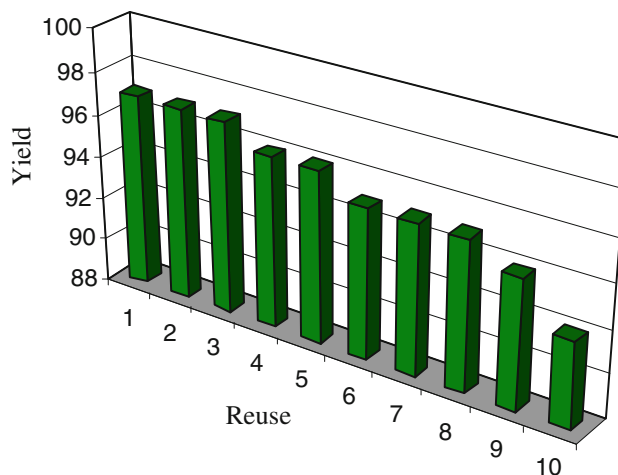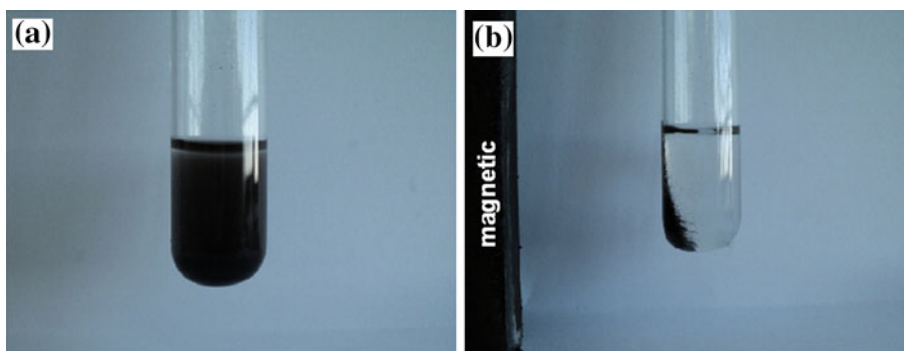
Fig. 6 Reuses performance of the catalysts

The catalytic activity of the Nano–$FeNi_3$–SiO_2 particles was compared with that of the Bulk–$FeNi_3$–SiO_2. For this purpose, the reactions were carried out separately at room temperature in water with both the catalysts for the appropriate time (Table 3). The aliquots of the reaction mixture were collected periodically at an interval of 5 min. Table 3 shows the variation of the percentage preparation of 4H-benzo[b]pyran with time, when Nano–$FeNi_3$–SiO_2 and Bulk–$FeNi_3$–SiO_2 were employed as catalysts. It is evident that, the catalytic activity of the Nano–$FeNi_3$–SiO_2 is much greater than that of the Bulk–$FeNi_3$–SiO_2. After 15 min, Nano–$FeNi_3$–SiO_2 showed 97 % preparation of 4H-benzo[b]pyran as compared to 36 % with Bulk–$FeNi_3$–SiO_2. The increased catalytic activity of Nano–$FeNi_3$–SiO_2 over the Bulk–$FeNi_3$–SiO_2 may be attributed to the higher surface area of SiO_2.

The catalytic activity of the $FeNi_3$–SiO_2 nanoparticles was compared with that of the Nano–SiO_2 and Nano–$FeNi_3$. For this purpose, the preparation of 4H-benzo[b]-pyran was carried out separately at room temperature in water with three nanoparticles. After 15 min, $FeNi_3$–SiO_2 nanoparticles and Nano–SiO_2 showed 97 % preparation of

Table 2 Effect of various catalysts and solvent conditions on the synthesis of 4H-benzo[b]pyran

Entry	Catalyst	Amount of catalyst (mol %)	Solvent	Temp (°C)	Time (min)	Yield[a] (%)
1	Na_2SeO_4	0.53	Water/EtOH (1:1)	Refluxed	60	97 [38]
2	Tetra-methyl ammonium hydroxide	10	H_2O	Room temperature	30–120	81 [39]
3	Nanosized $Ce_1Mg_xZr_{1-x}O_2$	34.8	EtOH	Reflux	35	91 [40]
4	NaBr	0.4	Neat	(MW)	10	95 [41]
5	MgO	0.5	Neat	Room temperature	10	75 [42]
6	$FeNi_3$–SiO_2	0.3	H_2O	Room temperature	15	97

[a] Isolated yields

Table 3 Comparison of the catalytic activity of Nano–$FeNi_3$–SiO_2 with Bulk–$FeNi_3$–SiO_2

Entry	Reaction time (min)	Yield (%)[a]	
		Nano–$FeNi_3$–SiO_2	Bulk–$FeNi_3$–SiO_2
1	5	76	23
2	10	85	28
3	15	97	36
4	20	97	41
5	25	97	41

[a] Isolated yields

4H-benzo[b]pyran as compared to 31 % with Nano–$FeNi_3$. The increased catalytic activity of $FeNi_3$–SiO_2 nanoparticles and Nano–SiO_2 over the Nano–$FeNi_3$ attributed to the higher surface area of SiO_2 and it is not arising from the leached [Fe] species into the solution.

As can be seen from Table 4, the reaction of aromatic aldehydes (compound 2) with malononitrile (compound 3) and 1,3-diketones (compound 1) at room temperature in water provided the corresponding 4H-benzo[b]pyran derivatives (compound 4) in good yields. The results are presented in Table 4 and indicate that aldehydes bearing electron-withdrawing groups react more quickly than their electron-donating aldehyde counterparts. For example, aromatic aldehydes such as 4-chloro, 4-nitro, and 4-bromo benzaldehydes react quickly with high-product yields in comparison to 4-hydroxy, 4-methyl, and 4-methoxy benzaldehyde derivatives. The yield of 4H-benzo[b]pyrans bearing group at ortho position on the aromatic ring is lower than that of the 4H-benzo[b]pyrans bearing group at para position on the aromatic ring (Scheme 2, Table 4).

On the other hand, when benzyl cyanide (compound 3′) was treated as a substitute for malononitrile in this reaction and under similar conditions, not only a highly prolonged time was required, but also the products were different. The

spectroscopic data of the products confirmed that these structures belong to octahydroxanthene (compound 5) (Scheme 3).

A mechanism for the reaction is outlined in Scheme 4. The reaction occurs via initial formation of the cyano olefin [A] from the condensation of aldehyde (1) and malononitrile (2), which reacts with 1,3-Diketone (3) to give the intermediate [B] which subsequently cyclises to afford the desired compound (4). The nano silica in the first step plays a key role in the cyclization process.

To further explore the potential of this protocol for heterocyclic synthesis, we investigated one-pot reactions involving 1,3-Diketone (compound 1), isatin (compound 7), malononitrile (compound 3), and obtained Spirooxindoles (compound 6) in excellent yields (Scheme 5, Table 5). A variety of isatin, both electron-donating and electron-withdrawing groups on the aromatic ring, were reacted with malononitrile and substituted 1,3-Diketones to generate Spirooxindoles (compound 6). As can be seen from Table 5, electronic effects and the nature of substituents on the aromatic ring did not show strong obvious effects in terms of yields under the reaction conditions. The three-component cyclocondensation reaction proceeded smoothly in water and was completed in 10–15 min; isatins containing electron-withdrawing groups or electron-donating were employed and reacted well to give the desired products in excellent yields with high purity.

To further expand the scope of this approach, we examined one-pot reactions involving acenaphthoquinone (compound 8), instead of isatin (compound 7). Under these conditions, a variety of desired spirochromenes (compound 9) was also produced in excellent yields (Scheme 6).

On the other hand, when ammonium acetate (compound 10) was treated as a substitute for malononitrile (compound 3) in this reaction and under similar conditions, not only a highly prolonged time was required but also the products were different. The spectroscopic data of the products confirmed that these structures belong to spiroacridine derivatives (compound 11a and b) (Scheme 7).
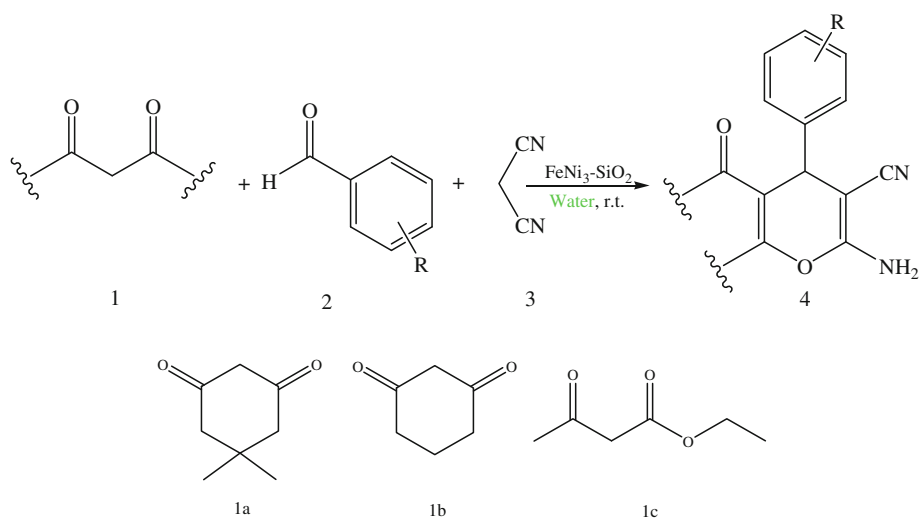
Table 4 Synthesis of 4H-benzo[b]pyran derivatives catalyzed by FeNi$_3$–SiO$_2$

| Entry	R	1,3-Diketone	Product	Time (min)	Yield (%)[a,b]	mp (°C)
1	C$_6$H$_5$	1a	4a	15	97	228–230 [43]
2	4-ClC$_6$H$_4$	1a	4b	10	98	207–209 [43]
3	2-Cl C$_6$H$_4$	1a	4c	15	96	135–137 [43]
4	4-MeC$_6$H$_4$	1a	4d	20	92	223–225 [43]
5	4-NO$_2$C$_6$H$_4$	1a	4e	10	97	179–180 [43]
6	2-NO$_2$C$_6$H$_4$	1a	4f	10	95	222–223 [44]
7	4-BrC$_6$H$_4$	1a	4g	10	95	200–202 [44]
8	2-BrC$_6$H$_4$	1a	4h	15	93	152–154 [44]
9	4-MeOC$_6$H$_4$	1a	4i	20	91	201–202 [43]
10	4-HOC$_6$H$_4$	1a	4j	20	92	205–206 [43]
11	4-FC$_6$H$_4$	1a	4k	10	97	192–194 [45]
12	4-Me$_2$NC$_6$H$_4$	1a	4l	20	91	199–201 [43]
13	C$_6$H$_5$	1b	4m	15	96	239–241 [46]
14	4-ClC$_6$H$_4$	1b	4n	10	97	226–229 [46]
15	2-ClC$_6$H$_4$	1b	4o	10	96	213–215 [46]
16	4-MeC$_6$H$_4$	1b	4p	20	92	214–216 [46]
17	4-NO$_2$C$_6$H$_4$	1b	4q	10	96	235–236 [46]
18	2-NO$_2$C$_6$H$_4$	1b	4r	10	94	196–198 [46]
19	4-MeOC$_6$H$_4$	1b	4s	20	92	193–195 [46]
20	4-HOC$_6$H$_4$	1b	4t	20	92	234–236 [46]
21	4-FC$_6$H$_4$	1b	4u	10	96	213–215 [46]
22	4-Me$_2$NC$_6$H$_4$	1b	4v	20	93	168–170 [46]
23	C$_6$H$_5$	1c	4w	15	96	193–195 [45]
24	4-ClC$_6$H$_4$	1c	4x	10	97	173–175 [45]
25	4-MeC$_6$H$_4$	1c	4y	20	92	180–182 [45]
26	4-MeOC$_6$H$_4$	1c	4z	20	91	140–142 [45]
27	4-NO$_2$C$_6$H$_4$	1c	4a′	10	98	183–185 [45]

[a] Reaction condition: benzaldehyde derivatives (1 mmol), 1,3-Diketones (1 mmol), malononitrile (1 mmol), FeNi$_3$–SiO$_2$ (0.0007 g) at room temperature in water
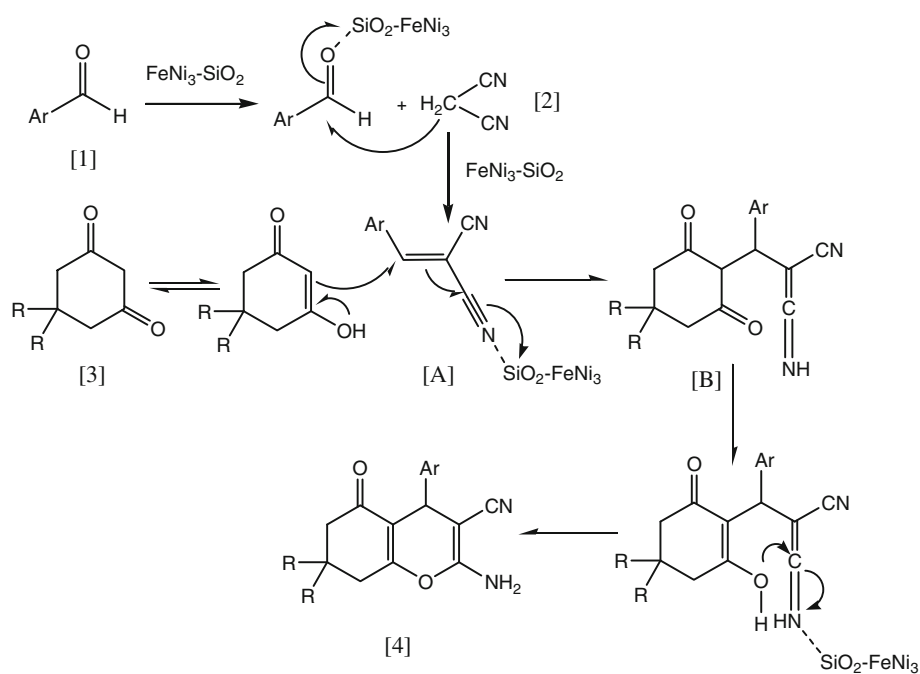
[b] Yield refers to isolated product

Scheme 2 Synthesis of derivatives 4 in the presence of FeNi$_3$–SiO$_2$

Scheme 3 Synthesis of
octahydroxanthene
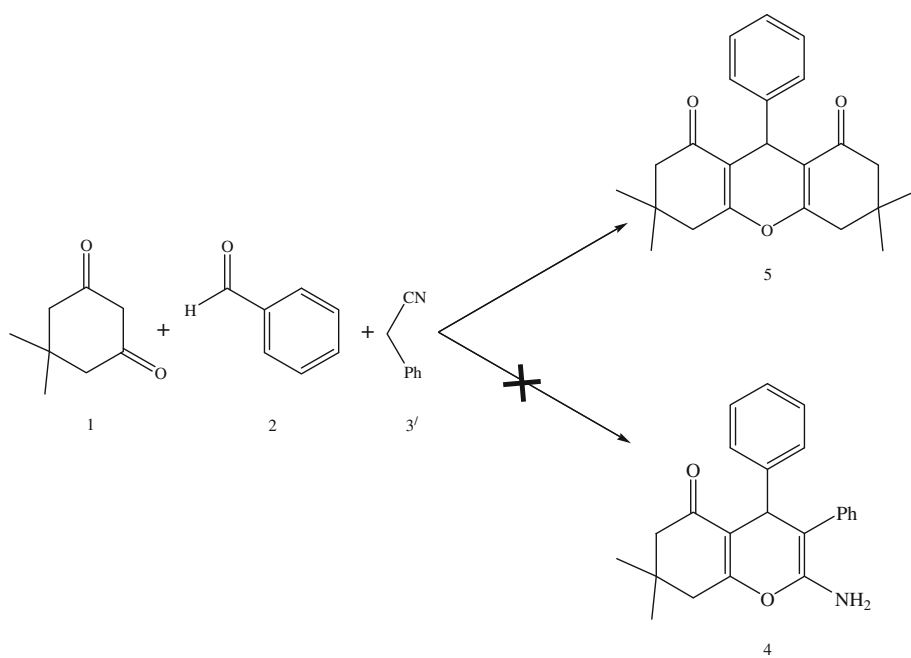
Scheme 4 Suggested
mechanism for the preparation
of 4H-benzo[b]pyrans

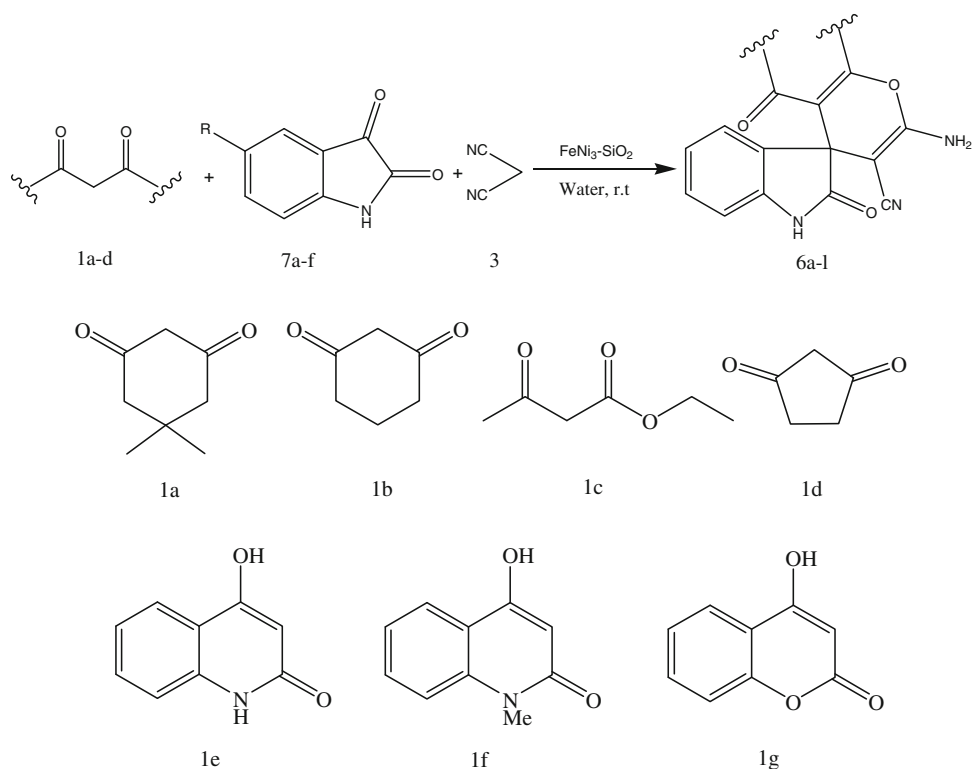**Scheme 5** Synthesis of Spirooxindoles derivatives 6 in the presence of Nano–SiO$_2$

Table 5 Synthesis of Spirooxindoles from malononitrile, 1,3-dicarbonyl compounds, and isatins

Entry	R	1,3-Diketone	Product	Time (min)	Yield (%)[a,b]	mp (°C)
1	H	1a	6a	15	96	>300 [47]
2	H	1b	6b	15	97	278–280 [48]
3	H	1d	6c	15	93	>300 [49]
4	H	1c	6d	15	95	271–273 [50]
5	H	1e	6e	15	94	>300 [51]
6	H	1f	6f	15	95	>300 [51]
7	H	1g	6g	15	93	>300 [51]
8	CH$_3$	1a	6h	10	92	275–278 [51]
9	Br	1d	6i	10	94	260–263 [51]
10	Cl	1d	6j	15	95	256–259 [51]
11	NO$_2$	1d	6k	10	95	270–272 [51]
12	OCH$_3$	1d	6l	15	92	217–219 [51]

[a] Conditions: isatin (1 mmol), 1,3-diketone (1 mmol), malononitrile (1 mmol), and water (5 mL)

[b] Isolated yields

Conclusions

In conclusion, the obtained results describe a novel, new, and simple method for the synthesis of 4H-benzo[b]pyrans and Spirooxindoles via one-pot, three-component reaction using FeNi$_3$–SiO$_2$ nanoparticles as catalyst at room temperature in water with high-product yields. This nanoparticle-based catalyst provides a new way for continuous processes, because of its simple recyclability. From a scientific point, our results expand the application of nanoparticles. This catalyst should be helpful to the development of new catalytic systems.

Scheme 6 Synthesis of spirochromenes using acenaphthoquinone
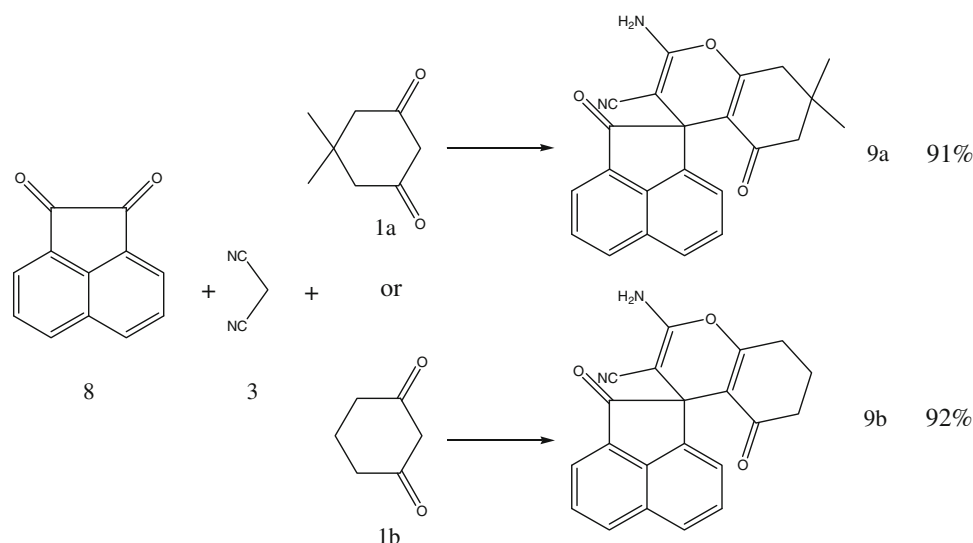
Scheme 7 Synthesis of spiroacridine
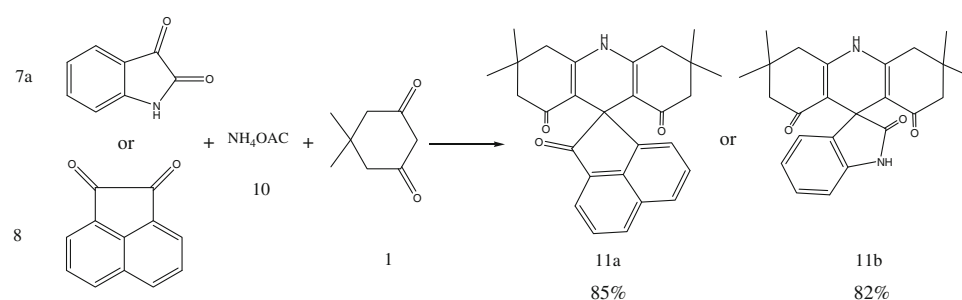
References

1. A.R. Katritzky, C.W. Rees, E.F.V. Scriven (Eds.), Pergamon Press: Oxford, **5**, 469 (1995)
2. W.O. Foye, Prinicipi di Chemico Farmaceutica; Piccin: Padova, Italy 416 (1991)
3. L.L. Andreani, E. Lapi, Bull. Chim. Farm. **99**, 583 (1960)
4. J. Skommer, D. Wlodkowic, M. Matto, M. Eray, J. Pelkonen, Leuk. Res. **30**, 322 (2006)
5. N. Yu, J.M. Aramini, M.W. Germann, Z. Huang, Tetrahedron Lett. **41**, 6993 (2000)
6. T.S. Jin, A.Q. Wang, X. Wang, J.S. Zhang, T.S. Li, Synletters 871 (2004)
7. D.Q. Shi, S. Zhang, Q.Y. Zhuang, S.J. Tu, H.W. Hu, Chin. J. Org. Chem. **23**, 877 (2003)
8. L.M. Wang, J.H. Shao, H. Tian, Y.H. Wang, B. Liu, J. Fluorine Chem. **127**, 97 (2006)
9. I. Devi, P.J. Bhuyan, Tetrahedron Lett. **45**, 8625 (2004)
10. S. Balalaie, M. Bararjanian, A.M. Amani, B. Movassagh, Synlett 263 (2006)
11. S.J. Tu, Y. Gao, C. Guo, D. Shi, Z. Lu, Synth. Commun. **32**, 2137 (2002)
12. J.T. Li, W.Z. Xu, L.C. Yang, T.S. Li, Synth. Commun. **34**, 4565 (2004)
13. Y. Penjg, G. Song, Catal. Commun. **8**, 111 (2007)
14. M. Dabiri, M. Bahramnnejad, M. Baghbanzadeh, Tetrahedron **65**, 9443 (2009)
15. Y.R. Lee, G.S. Hari, Synthesis **3**, 453 (2010)
16. L.M. Wang, N. Jiao, J. Qiu, J.J. Yu, J.Q. Liu, F.L. Guo, Y. Liu, Tetrahedron **66**, 339 (2010)
17. L. Yuling, C. Hui, S. Chunling, S. Daqing, J. Shunjun, J. Comb. Chem. **12**, 231 (2010)
18. S.-L. Zhu, S.-J. Ji, Y. Zhang, Tetrahedron **63**, 9365 (2007)
19. R. Sridhar, B. Srinivas, B. Madhav, V.P. Reddy, Y.V.D. Nageswar, K. Rao, R. Can, J. Chem. **87**, 1704 (2009)
20. E.G. Deroune, G. Crehan, C.J. Dillon, D. Bethell, H. He, S.B.D. Hamid, J. Catal. **194**, 410 (2000)
21. C. Li, H. Huang, S. Yang, R. Zheng, W. Yang, Z. Lio, S. Ringer, Mater. Lett. **63**, 1016 (2009)
22. I. Tkac, P. komadel, D. MullerI, Clay Miner. **29**, 101 (1991)
23. G.D. Yadav, J.J. Nair, Micropor. Mesopor. Mater. **33**, 1 (1999)
24. J.R. Sohn, M.Y. Park, Appl. Catal. **101**, 129 (1993)
25. A. Cornelis, A. Gertsman, P. Laszlo, I. Zicba, Catal. Lett. **6**, 103 (1990)
26. C. Cativiela, J.I. Garcia, M.G. Matres, B. Chiche, Appl. Catal. **123**, 273 (1995)
27. L.P. Davila, V.J. Leppert, E.M. Bringa, Scripta Mater. **60**, 843 (2009)
28. S.-E. Park, Sujandi. Curr. Appl. Phys. **8**, 664 (2008)
29. J.L. Gole, M.G. White, J. Catal. **204**, 249 (2001)
30. J.M. Thomas, R. Raja, Chem. Record **1**, 448 (2001)
31. M. Sadeghi, M.A. Semsarzadeh, H. Moadel, J. Member. Sci. **331**, 21 (2009)
32. G.D. Yadav, Catal. Surv. Asia **9**, 117 (2005)
33. M.L. Kantam, S. Laha, J. Yadav, B. Sreedhar, Tetrahedron Lett. **47**, 6213 (2006)
34. M.-J. Kim, W.-H. Kim, K. Han, Y.K. Choi, J. Park, Org. Lett. **9**, 1157 (2007)
35. J.S. Lu, Nanomat. **1** (2006)
36. C.W. Lim, I.S. Lee, Nano Today **5**, 412 (2010)

37. X. Lu, G. Liang, Q. Sun, C. Yang, J. Alloy. Compd. **509**, 5079 (2011)
38. R. Hekmatshoar, S. Majedi, K. Bakhtiari, Catal. Commun. **9**, 307 (2008)
39. S. Balalaie, M. Sheikh-Ahmadi, M. Bararjanian, Catal. Commun. **8**, 1724 (2007)
40. S. Rathod, B. Arbad, M. Lande, Chin. J. Catal. **31**, 631 (2010)
41. I. Devi, P.J. Bhuyan, Tetrahedron Lett. **45**, 8625 (2004)
42. D. Kumar, V. Buchi Reddy, S. Sharad, U. Dube, S. Kapur, Eur. J. Med. Chem. **44**, 3805 (2009)
43. L. Fotouhi, M.M. Heravi, A. Fatehi, K. Bakhtiari, Tetrahedron Lett. **48**, 5379 (2007)
44. R. Hekmatshoar, S. Majedi, K. Bakhtiari, Catal. Commun. **9**, 307 (2008)
45. D. Kumar, V.B. Reddy, S. Sharad, U. Dube, S. Kapur, Eur. J. Med. Chem. **44**, 3805 (2009)
46. S. Rathod, B. Arbad, M. Lande, Chin. J. Catal. **31**, 631 (2010)
47. K. Gong, H. Wang, J. Luo, Z.L. Liu, J. Heterocycl Chem. **46**, 1145 (2009)
48. F.F. Abdel-Latif, M.M. Mashaly, E.H. El-Gawish, J. Chem. Res. **5**, 1220 (1995)
49. K.C. Joshi, A. Dandia, S. Baweja, A.J. Joshi, Heterocycl. Chem. **26**, 1097 (1989)
50. L.M. Wang, N. Jiao, J. Qiu, J.J. Yu, J.Q. Liu, F.L. Guo, Y. Liu, Tetrahedron **66**, 339 (2010)
51. K. Rad-Moghadam, L. Youseftabar-Miri, Tetrahedron **67**, 5693 (2011)